

Article

The Chinese Aviation Network: An Empirical Temporal Analysis on Its Structural Properties and Robustness

Ruoshi Yang ¹, Wei Sun ², Meilong Le ^{1,*} and Hongyan Zhang ²

¹ College of Civil Aviation, Nanjing University of Aeronautics and Astronautics, Nanjing 210016, China; yangruoshi@nuaa.edu.cn

² School of Information Science and Technology, Hainan Normal University, Haikou 571158, China; cs.weisun@foxmail.com (W.S.); hongyan@hainnu.edu.cn (H.Z.)

* Correspondence: lemeilong@126.com; Tel.: +86-13918976990

Abstract: Complex networks have encouraged scholars to develop an effective method for abstracting and optimizing aviation networks. However, researchers often overlook the aviation network's temporal attribute and treat it as a static network. Aviation networks have strong temporal characteristics and the dynamic connection cannot be realistically described by a static network. It is necessary to more accurately and realistically represent these connections during the operation of an aviation network. This study explored temporal structures of the Chinese aviation temporal network (CATN) based on flight schedules and actual operational time data. Temporal networks based on time windows were represented to analyze the temporal topology features and robustness of the CATN. The results demonstrated the following: (1) based on the spatial-temporal aviation network, there is a morning departure peak (7:00–8:00) and an evening arrival peak at the airline hub (20:00–21:00); (2) examining the centrality of each airport in the CATN at various time intervals exposed fluctuations in their rankings, which could not be identified by a static network, and (3) the robustness of the CATN was found to be unaffected by time windows, but it displayed poor resilience against deliberate attacks, particularly when subjected to betweenness and closeness attacks, which target the network's shortest paths. For obtaining a greater understanding of the operating situation of civil aviation, displaying the topological features and robustness of the temporal network is of great importance.

Keywords: Chinese aviation temporal network; temporal network; topological structure; complex networks, robustness



Citation: Yang, R.; Sun, W.; Le, M.; Zhang, H. The Chinese Aviation Network: An Empirical Temporal Analysis on Its Structural Properties and Robustness. *Appl. Sci.* **2023**, *13*, 11627. <https://doi.org/10.3390/app132111627>

Academic Editors: José Balthazar, Angelo Marcelo Tusset, Átila Madureira Bueno and Diego Colón

Received: 20 September 2023

Revised: 20 October 2023

Accepted: 21 October 2023

Published: 24 October 2023



Copyright: © 2023 by the authors. Licensee MDPI, Basel, Switzerland. This article is an open access article distributed under the terms and conditions of the Creative Commons Attribution (CC BY) license (<https://creativecommons.org/licenses/by/4.0/>).

1. Introduction

The aviation network functions as a typical complex system, with its subsystems that interact to generate functionality rather than being created by a specific subsystem [1–3]. Complex network theory enhances our understanding of the functionality and behavior of the aviation transportation system. The aviation network consists of nodes and edges, with nodes that represent airports or cities where airports are located and edges that represent connections between airports [4]. To model the US aviation network, Li-Ping [5] utilized a directed weighted network and analyzed its degree distribution and clustering coefficient. Li and Cai [6] analyzed the Chinese aviation network (CAN) with 128 airport nodes and 1165 flights, and found that its average shortest path was 2.067 and its clustering coefficient was 0.733, indicative of a small-world network classification. Barrat [7] examined the global aviation-weighted network and investigated the correlation between weight and the underlying topological structures of the network. Gautreau [8] analyzed the interaction between macroscopic and microscopic airport network characteristics in the US. Empirical studies demonstrate that both Chinese and global aviation networks have small-world properties, with short average shortest paths and high clustering coefficients.

Both networks exhibit a double power-law distribution pattern in their respective degree distributions [9–12].

The majority of studies on aviation networks have concentrated on examining their static structures, overlooking the correlations present across various time periods. In static networks, the relationship between nodes depends only on the existence of a flight route, which disregards any temporal data such as departure and arrival times or delays. This oversimplified static abstraction leads to overestimating the connections among nodes and distorts the understanding of the system's structure. Temporal networks are characterized by the connections among nodes which vary over time periods [13]. Integration of the time dimension into the network model results in more complex interrelationships and presents novel challenges to static network theory.

Early researchers described temporal networks using weighted networks, with edge weight signifying the number of incidences over the entire time period. Nevertheless, this model considers an impractical assumption that the connections between pairs of nodes are randomly distributed within the time period [14]. To evaluate the presence of directed edges between nodes and to establish reachability graphs, Moody et al. [15] introduced the concept of temporal reachability. However, this model is only suitable for sparse networks. To overcome this drawback, several studies [16,17] discretized aggregated temporal networks into snapshot sequences using time windows, where the interactions between nodes within a time window belong to the same time window, and each snapshot within the time window is independent of the others. By correctly mapping temporal networks into static networks, the research characterized changes in network features such as the degree, betweenness, and clustering coefficient. Although these methods are broadly accepted in temporal network research, the selection of an appropriate time window size remains a crucial challenge. A small time window setting results in numerous invalid empty network structures, whereas using the entire observation window as the time window renders the temporal network static, leading to the loss of temporal information. Furthermore, these models ignore continuity in time when the interaction between nodes spans multiple time windows, resulting in inaccurate temporal information.

In recent years, there has been a growing trend among scholars to utilize temporal networks for the aviation transportation network. Ralvi et al. [18,19] captured the complexity within specific time windows and introduced corresponding complexity metrics to understand the dynamic evolution of complexity within these windows. Moreover, they introduced the concept of individual aircraft complexity to assess individual contributions and proposed a method for defining complex communities that evaluate the impact of various decisions on the overall system. To better represent the temporal relationship between flights, Mikko et al. [20] integrated temporal networks into the event graph framework to investigate the characteristics of these networks. Humberto and Lilian [21] analyzed the robustness of temporal networks in light of this framework.

This study aimed to model the CAN as a temporal network and to analyze its temporal topology to better understand the structural characteristics that determine the network's resistance to random and deliberate attacks. The researchers analyzed the robustness of the Chinese aviation temporal network (CATN) and provided insights into the obtained results. The remainder of the paper is organized as follows: Section 2 presents the methods used for building and researching the CATN. In Section 3, the theory of temporal networks was utilized to conduct an empirical analysis of the CATN. Section 4 further investigates the robustness of the temporal network model. The conclusions of the research are presented in Section 5.

2. Modeling and Research Methods

This study employed complex networks as a modeling tool to capture the dynamic behavior of the CATN and investigated its properties. Robustness measurements were utilized to quantify the network's structure and its ability to withstand potential disruptions.

2.1. Modeling the CATN

A temporal network refers to a system in which clear time evolution and temporal characteristics are evident [22,23]. In this system, nodes may emerge or vanish during the process of temporal changes, and interactions among nodes may appear or disappear with the progress of time. This study proposed an aggregated network $G = (V_G, E_G, T)$ to represent the temporal network. In this method, V_G defines a set of nodes, and E_G denotes a set of edges interacting within a finite time period of $[0, T]$. Each edge is represented with a quadruplet $e = (i, j, t, \Delta t)$, where i and j serve as node identifiers, t stands for the time of interaction, and Δt signifies the duration of connectivity. Although the implementation of static network visualization for the temporal network may yield improved visualization results, this approach does not fully incorporate topological and temporal information.

Ferreira [24] suggested the use of time windows to transform interactions that take place during the same time window into a static graph. A snapshot-based temporal graph [25] can map dynamic temporal aggregation networks (G) to a time sequence of static graphs (G_1, G_2, \dots, G_n) . This method assists us in processing temporal information contained in the network's quadruplets. By defining time windows symbolized by ω , a temporal network with $N = |V_G|$ nodes and duration T can be efficiently divided into $L = \frac{T}{\omega}$ snapshots. In this scenario, L signifies the number of snapshots obtained after the division. Each snapshot captures either all the events that occur within a specific time window or events that occur at a precise moment in time, with the collected information that characterizes these events.

In the framework of the CATN, a temporal network can be established by utilizing a triplet $e = (i, j, t)$ based on flight schedules. In this notation, i and j denote the departure and arrival airports of the flight, respectively, while t indicates its departure time. Figure 1a shows a snapshot of the aggregation network, which consists of five airports and flights. Time information indicates that the departure time at t is available on the edges. By utilizing a time window of $\omega = 1$ or $\omega = 2$, one can generate temporal snapshot sequences (see Figure 1b,c).

2.2. Temporally Topological Measures

The aggregated temporal network and snapshot-based temporal network are two methods for mapping dynamic temporal networks into static networks. Scholars have proposed numerous concepts and models for studying the topological properties of static networks. These methods can, to some extent, reflect the topological structure of the temporal network and have been extensively employed for various forms of air transportation networks [26–29]. A novel technique has been introduced for researching the structure of temporal topology, which is based on a static graph. A network is an undirected weighted graph $G(t)$ with nodes and edges varying across time periods of $t \in \{1, 2, \dots, t, \dots\}$. $V(t) = \{v_1(t), v_2(t), \dots, v_n(t)\}$ represents the set of nodes in time period t , and each node represents an airport, with a total of $N = |V(t)|$. $E(t) = \{e_1(t), e_2(t), \dots, e_m(t)\}$ represents the set of routes between airports, and there are $M = |E(t)|$ routes during t . Each edge $e_i(t)$ connects airports a and b . Thus, an $N \times N$ adjacency matrix, $A(t)$, is associated with the undirected weighted graph, in which A_{ij} is equal to 1 when there is a route between nodes i and j ; otherwise, A_{ij} will be equal to 0.

2.2.1. Node Degree and Distribution

The degree of each node $v(t) \in V(t)$, denoted as $d(t, v)$, is defined as the number of edges that connect to it. To calculate the degree of a given node $v(t)$, the adjacency matrix $A(t)$ can be utilized. If the v th row of $A(t)$ indicates the adjacent nodes to node v , then the degree of node v can be obtained using the following equation:

$$d(t, v) = \sum_{i=1}^n A_{vi}(t) \quad (1)$$

where $A_{vj}(t)$ indicates whether there is at least one flight between nodes v and j at time t , and is equal to 0 if there are no flights that connect them.

The temporal average degree of a network refers to the average number of edges connecting each node in the network at a given time t . Higher average degrees in a network imply that nodes within this network are more likely to be interconnected, resulting in higher overall network connectivity. A mathematical formula for the temporal average degree is as follows:

$$\bar{d}(t) = \frac{1}{N} \sum_{i=1}^n \sum_{j=1}^n A_{ij} \tag{2}$$

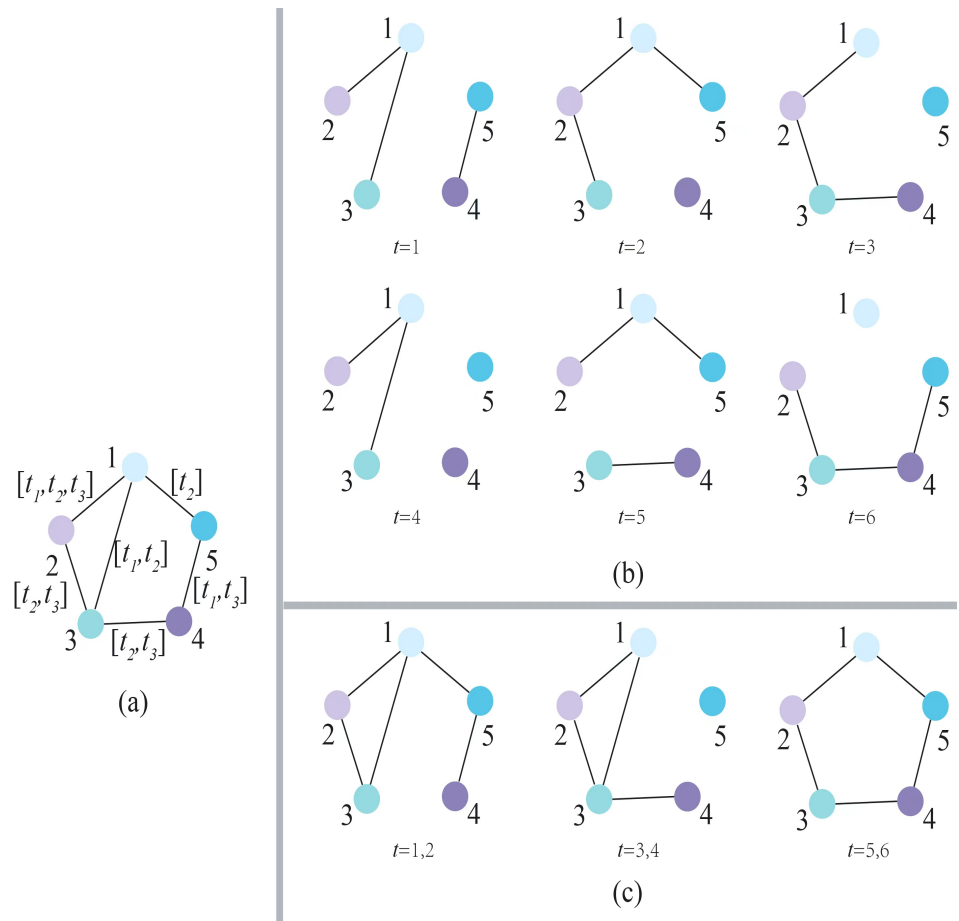


Figure 1. Different forms of instantaneous undirected networks: (a) an aggregated network, (b) a snapshot-based temporal network with a time window of 1 based on graph (a), and (c) a snapshot-based temporal network with a time window of 2 based on graph (a).

2.2.2. Temporal Average Path Length

The temporal average path length $L(t)$ refers to the average number of edges that connect any two nodes i and j in a network at a given time t . For pairs of nodes with no connection, their path length is defined as infinity. The following formula can be used to calculate $L(t)$:

$$L(t) = \frac{1}{N(N-1)} \sum_{i \neq j} l_{ij}(t) \tag{3}$$

where $l_{ij}(t)$ symbolizes the shortest path length between nodes i and j at time t . In an airline network, it represents the average number of transfers needed for any node to reach its final destination.

2.2.3. Clustering Coefficient

The clustering coefficient measures the possibility of two neighboring nodes being connected, and it is defined as the ratio of the actual edges between them to the number of all possible edges. The clustering coefficient quantifies the strength of intra-cluster connectivity and characterizes the closeness between nodes within a network. In particular, the clustering coefficient $C(t, v)$ of a given node $v(t)$ is computed using a function of the number of edges n_e among its neighbors and $d(t, v)$, which is the degree of node $v(t)$. The function is defined as

$$C(t, v) = \begin{cases} \frac{2n_e}{d(t, v)(d(t, v) - 1)} & \text{if } d(t, v) > 1 \\ 0 & \text{otherwise} \end{cases} \quad (4)$$

Note that, in the above equation, the condition $d(t, v) > 1$, indicates that the node $v(t)$ is connected to two or more neighboring nodes, while $\frac{d(t, v)(d(t, v) - 1)}{2}$ represents the number of potential edges in the network. If the node $v(t)$ has less than or equal to one neighbor, then its clustering coefficient is equal to zero.

The average clustering coefficient $C(t)$ in a network is defined as the mean of all node clustering coefficients. It can be calculated as follows:

$$C(t) = \frac{1}{N} \sum_{i=1}^n C(t, i) \quad (5)$$

The clustering coefficient characterizes the density of a network and the inter-connection of nodes. A high clustering coefficient indicates a dense network with closely connected nodes, while a low clustering coefficient implies a sparser network with less connectivity between nodes.

2.2.4. Strength

During operational processes, aviation network traffic distribution is often non-uniform. The strength of a node is usually represented by the sum of the routes or flights. Weighted networks can be implemented to better represent and monitor such traffic. Temporal networks, likewise, can also be represented as undirected weighted graphs $G(t) = (V(t), E(t), w)$, where $V(t)$ and $E(t)$ have the same definitions as in undirected unweighted networks previously described. The function $w : E(t) \rightarrow \mathbb{R}$ maps the set of edges to the real number set \mathbb{R} and denotes the weight of each edge. The adjacency matrix is defined by the following equation:

$$A_{ij}(t) = \begin{cases} w(i, j) & \text{if } (i, j) \in E(t) \\ 0 & \text{otherwise} \end{cases} \quad (6)$$

2.3. Robustness

The concept of network robustness is measured by the capability of a given network to continue to be connected, despite the failure or attack of a vertex [30]. Two main factors contributing to this problem are network attack strategies and the measurement of robustness.

2.3.1. Attack Strategies

Network attack methods can be categorized as either random failure or deliberate attack [31,32]. In aviation networks, random destruction resulting from non-subjective factors, such as the operation status of internal and external infrastructure within the aviation system and occasional extreme weather conditions, is classified as a random failure. The Rand function was utilized to generate random numbers, and the authors then applied the function that removes airport nodes and routes randomly. The network's

performance was measured following the attack until the metric was smaller than or equal to the predetermined threshold. Exploring the effects of random failure and deliberate attacks is vital in understanding the resilience of a network and can guide the development of more efficient security mechanisms for network protection.

In addition to objective factors such as weather and equipment, the aviation network is also vulnerable to various forms of subjective interference, often in the form of biased attacks where critical nodes with higher importance are prioritized as preferred targets. The importance of a node depends on the extent of the decline in connectivity of the airline network following an attack. To assess node importance, centrality is utilized in deliberate attacks. This study employed four types of centrality, namely degree centrality (the number of connections between nodes), the nearest neighborhood degree centrality (local clustering measure), betweenness centrality (the extent of the node used as an intermediary between other nodes), and closeness centrality (the average distance between a node and all other nodes in the network). Formulas (7)–(10) show the computational methods for these centrality types, respectively:

$$C_D(t, v) = d(t, v) \tag{7}$$

where $d(t, v)$ refers to the degree of node v at time t , i.e., the number of edges connected to node v at time t .

$$C_{D_{nn}}(t, v) = \frac{\sum_{i \in N_i} d(t, i)}{d(t, v)} \tag{8}$$

where N_i represents the set of neighboring nodes of node i .

$$C_B(t, v) = \sum_{\substack{i=1 \\ i \neq v}}^n \sum_{\substack{j=1 \\ j \neq v}}^n \frac{\sigma_{ij}(t, v)}{\sigma_{ij}(t)} \tag{9}$$

where $\sigma_{ij}(t)$ stands for the number of shortest paths from node i to node j at time t , while $\sigma_{ij}(t, v)$ signifies the number of such paths that pass through node v .

$$C_C(t, v) = \frac{N - 1}{\sum_{\substack{i=1 \\ i \neq v}}^n l_{vi}(t)} \tag{10}$$

where $l_{vi}(t)$ is the length of the shortest path from node i to node v at time t .

2.3.2. Robustness Measurement

Initially, scholars typically used network performance parameters to evaluate network robustness. These parameters included the number of connected components, the maximum component size, the network diameter, the average shortest path length, the network efficiency, the clustering coefficient, and numerous centrality indicators. These indicators provide different perspectives for measuring network robustness and therefore necessitate tailored measures to be taken based on the specific problems that need to be addressed. Network efficiency and the maximum connected sub-graph proportion were used as measures of robustness.

In case a network is subjected to continuous attack, the size of the maximum connected sub-graph becomes an indispensable measure of network performance. It displays the maximum connected component that separates from the network after the attack and reflects the network connectivity. The size of the maximum connected sub-graph relative to the original network determines the proportion of retained nodes after an attack. A smaller value indicates more substantial damage to the network. The relative size can be evaluated using the following relation:

$$S(t) = \frac{N_{live}}{N} \tag{11}$$

where $N_{\text{live}}(t)$ stands for the number of nodes preserved in the maximum connected sub-graph following the network attack at time t , while n symbolizes the total nodes in the original network at time t .

Latora [33] defined global efficiency, also known as network efficiency in this reference, as the average value of the reciprocal distances between all node pairs in a network. It indicates the convenience or difficulty of accessing one node from another, making it a fundamental measure of network connectivity. The calculation formula for global efficiency is as follows:

$$E(t) = \frac{1}{N(N-1)} \sum_{i \neq j} \frac{1}{l_{ij}(t)} \tag{12}$$

where n refers to the number of nodes in the network at time t , and $l_{ij}(t)$ signifies the shortest distance between node i and node j at time t .

3. Empirical Analysis

3.1. Flight Data

Our research utilized data on all domestic flights in China for the year 2018, obtained from VariFlight, the leading aviation data service provider in China. Flights from Hong Kong, Macau, and Taiwan regions were excluded. These data included the most extensive information regarding the number of flights and airports in China during that year. The data consist of 11 valid attributes that are presented in Table 1. The redundancy of some redundant variables, which were not related to our research objectives, could not be used in our research and could potentially affect data processing speed. To address this issue, the researchers removed the delay information.

Table 1. Description of Data.

Variable Type	Variable Name
Time Information	Departure time information: Scheduled departure time, Actual departure time
	Arrival time information: Scheduled arrival time, Actual arrival time
Delay Information	Departure delay in seconds
Airport Information	Landing airport information: Airport IATA code
	Take-off airport information: Airport IATA code
	Airport location information: Airport Longitude, Airport Latitude, Province, City

During the process of collecting, storing, and retrieving data, missing values, outliers, or inconsistencies are often encountered. To ensure the accuracy and effectiveness of the data, it is necessary to analyze the missing values, outliers, and duplicates to determine the validity of the data. The authors dealt with the data that had undergone attribute processing. These data contained a total of 4,961,074 data entries, standing for the total number of flights in 2018. Of the 35,715 records, 0.07% had missing actual take-off and landing times. The purpose of processing the data was to create a temporal network. While constructing the network, this study had to consider the following constraints: the departure time of the flights is after 4:00 a.m. in the morning, and the landing time is before 4:00 a.m. the following day. Only data that met these conditions were defined as valid data.

A considerable amount of data in our available data was either missing, invalid, or redundant. Therefore, it was vital to conduct data preconditioning before data mining to improve data quality and satisfy the application requirements. The primary and most fundamental method to deal with missing data is to eliminate the samples that contain missed data. The existing data were mostly affected by missing values in actual takeoff and landing times. Upon comparison with actual operational data, it became evident that the presence of missing values was often observed in conjunction with distinct situations, such as diversion or midair returns. As a result, the missing data points were deemed invalid.

Apart from missing values, data validity needed to be assessed. Hence, to comply with the aforementioned constraints, the researchers had to remove data collected before 4:00 a.m. on 1 January 2018, because they are not classified as belonging to 2018. In addition, the data between 0:00 and 4:00 a.m. on 1 January 2019, were not available, so the researchers removed data between 4:00 a.m. on 30 December 2018 and 0:00 on 31 December 2018 to ensure data accuracy (Data from the year 2018 are inclusive of 1 January 2018, from 4:00 a.m. to 31 December 2018, until 4:00 a.m.). After the completion of the data preprocessing phase, a total of 4,915,350 valid data records were obtained. These records represent 99.08% of the initial dataset.

3.2. Topological Properties of the CATN

The CATN contains all flights that took place within China, excluding Hong Kong, Macao, and Taiwan, during the year of 2018. Each flight was defined by a quadruplet $(i, j, t, \Delta t)$, where i and j indicate the departure and arrival airports, respectively, t denotes the departure time, and Δt stands for the elapsed time from arrival to departure. By aggregating data from all the flights during 2018, the CATN could be expressed as a temporal network that included 230 airport nodes (i.e., $N = 230$) and a total of 3880 weighted edges that had time labels (i.e., $|E| = 3880$). Figure 2 exhibits an intuitive illustration of the CATN's configuration.

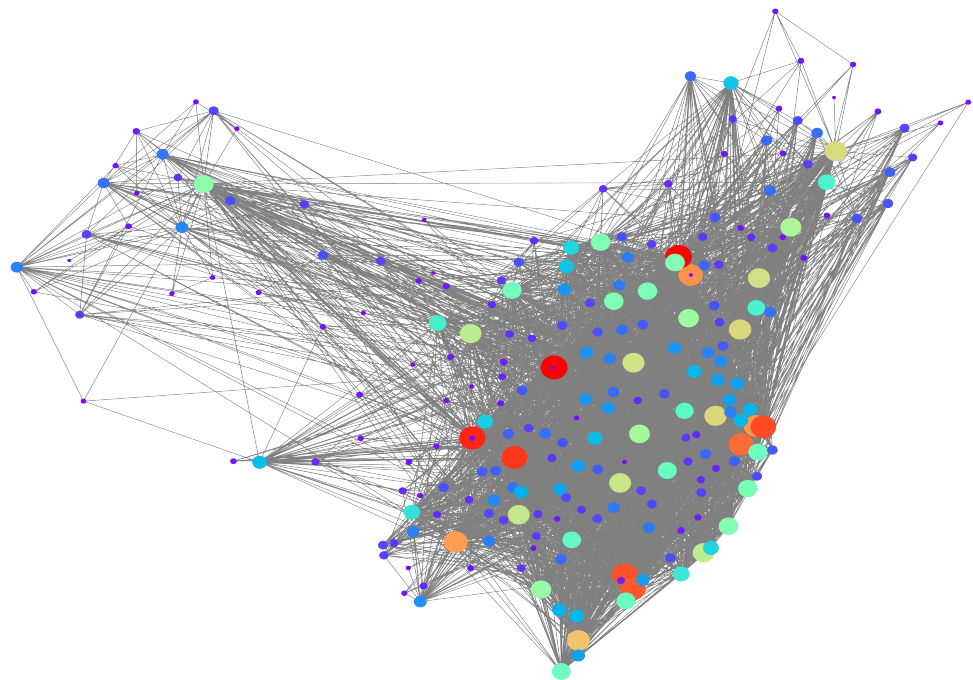


Figure 2. The CATN was constructed solely based on domestic civil aviation transport within China in 2018. The node's size and color stand for their respective degree, and the edges provide temporal information.

The presence of non-numerical time data stored at the edges of a temporal network makes it unsuitable for static network exploration. To avoid this situation, the authors used a snapshot-based temporal network model to investigate the topological features of dynamic networks. Our model partitioned time into hourly intervals, with a window of ω at one hour, and an overall aggregating time span of T from 1 January 2018 at 4:00 a.m. to 31 December 2018 at 4:00 a.m., which resulted in the generation of 8760 snapshot networks. Our dynamic network model can thus be regarded as a sequence of static networks, in which each snapshot is analyzed to explore the topological and temporal characteristics of the CATN.

3.2.1. Temporal Attributes of Nodes and Edges

The temporal variation of China’s airline routes throughout 2018 is displayed in Figure 3. The number of airlines in the Chinese airline network sharply increased at 6:00 and suddenly decreased at 10:00. The primary operational time of the overall network was from 6:00 to 24:00, such that 99% of flights in 97% of airports occurred during this time period. Peaks in flights occurred at 07:00 and 10:00, with each displaying an average number of flights of 510 and 530, respectively. These peaks signify a limitation in the operational capacity of the overall civil aviation network. The network was weighed based on the number of flights in each time period to investigate the changes in flight schedules, resulting in similar findings to those of the unweighted network. Unlike urban transportation, air transportation experiences long periods of sustained peak traffic [34].

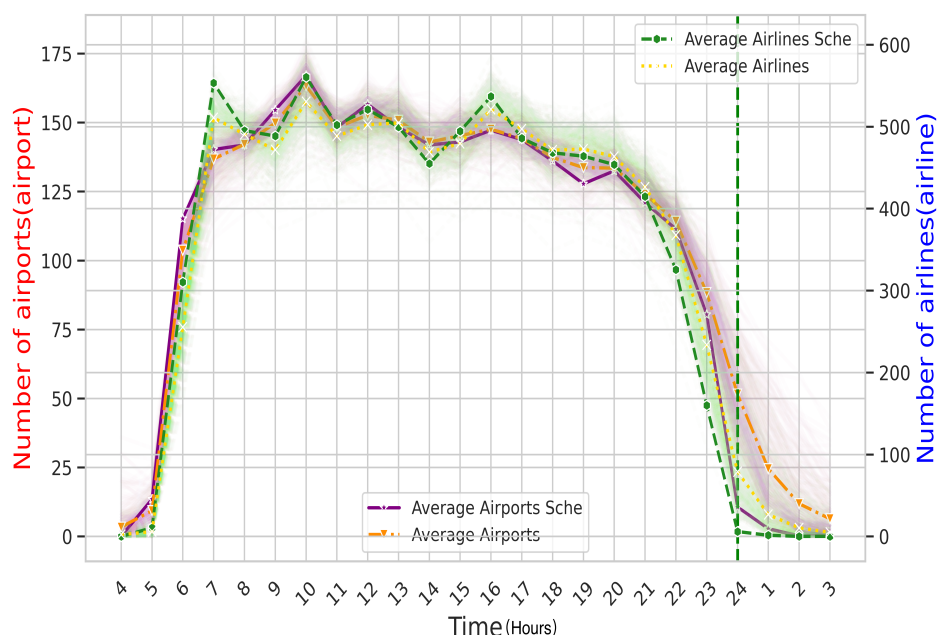


Figure 3. The presented graph depicts the temporal evolution of the number of airports and flight routes in the CATN. The yellow and green lines correspond to the average number of planned and actual flight routes per time period, whereas the purple and orange lines indicate the average number of planned and actual airports. The shaded regions of diverse colors illustrate the fluctuation of daily actual data around the mean value.

According to regulations of the Civil Aviation Administration, domestic airlines are advised to reduce the number of “red-eye flights”, which are flights that depart and arrive after midnight. On average, there are fewer than 10 flights per day (0.1% of the total) that are scheduled to take off after midnight in the flight schedule, but in actual operations, an average of 94 flights per day (3% of the total) take off after midnight. To further explore this phenomenon, the authors analyzed the flight schedule by dividing time into hourly intervals based on scheduled departure time (Figure 4). The chart clearly shows that almost no flights are scheduled to take off after midnight in the Civil Aviation Administration’s flight schedules. The researchers calculated the difference between the scheduled and actual number of flights for each hour of the year and found that there were discrepancies between 5:00 and 12:00 and between 15:00 and 16:00. This deviation led to flight delays and an increase in the number of “red-eye flights” in operation. However, during other times, the actual number of flights exceeded scheduled estimates, suggesting that airlines handled abnormal flights during those periods.

This study evaluated representative airports of various types, including domestic slot-coordinated airports such as Beijing Capital International and Xi’an Xianyang International, gateway airports such as Urumqi Diwopu International and Kunming Changshui

International, and provincial airports such as Lanzhou Zhongchuan International. Through examining the number of flights over time (Figure 5), the authors identified significant peak periods of outbound flights for Beijing, Xi’an, and Kunming, with values that dropped noticeably after 10:00. This suggested ample capacity at the operations, airspace, runways, and other support resources that could redistribute flights via ground wait and flow control after 10:00. However, Urumqi and Lanzhou had stable values, implying that their support resources such as runways and airspace were nearing saturation.

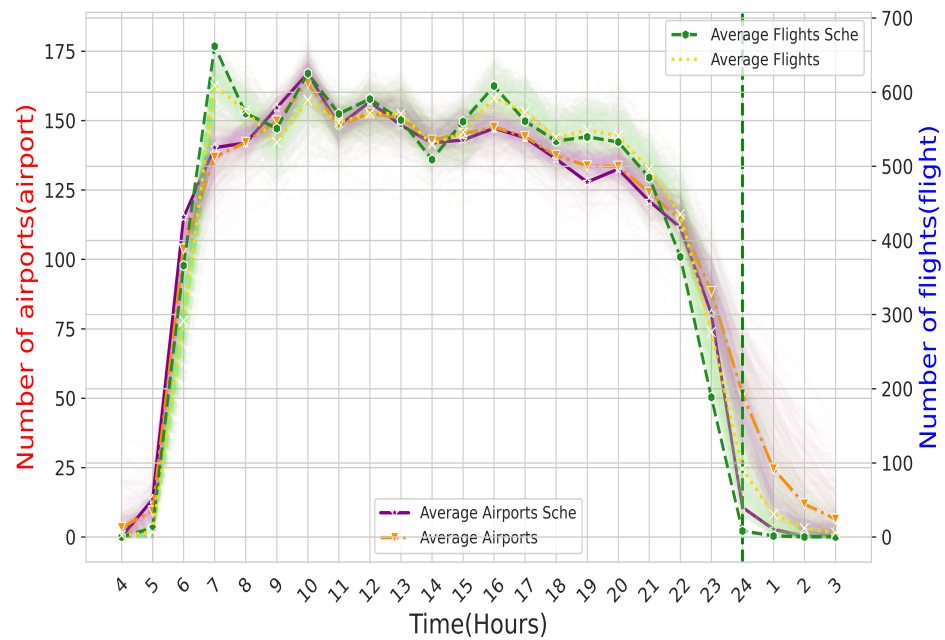


Figure 4. The presented figure showcases the changes in the hourly counts of airports and flights in the CATN. Specifically, the green and yellow lines correspond to the actual and planned average count of flights, respectively, for each time period. Equivalently, the purple and orange lines represent the actual and planned average count of airports, respectively, for each time period. Various shaded regions of divergent colors correspond to daily actual data that fluctuate around the mean.

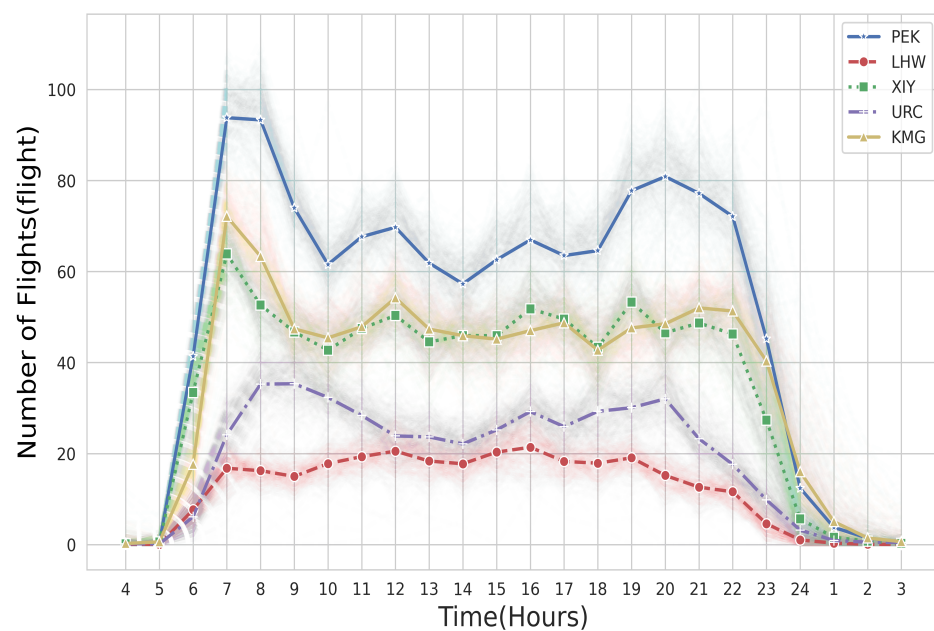


Figure 5. Flight volumes at specific airports over time.

Overall, the temporal variation of airline routes and flights in China highlights the challenges in the operational capacity of the CATN, particularly in handling peak traffic. These limitations lead to flight schedule delays, and airports resort to scheduling “red-eye flights” to accommodate all daily flights, consequently increasing the risk of aviation operations. Furthermore, evaluations of various representative airports reveal that they continue to encounter these constraints, although their operational capacities vary. Therefore, when developing flight optimization plans, it is crucial to optimize them based on the distinct operational capacities of different airports.

3.2.2. Temporal Property of Node Degree

Node degree changes over time partially reflect the temporal characteristics of airport operation. Based on the CTAN constructed on 1 October 2018, the spatiotemporal characteristics of the air transportation network were illustrated at 6:00, 12:00, 18:00, and 24:00 by integrating the spatial information of airports’ locations. The results revealed that, from 6:00 to 7:00 in the morning, routes were sparse with a small number of travelers, and most departures were from economically developed cities (Figure 6). After 8:00, a significant number of small and medium-sized airports joined the network and aggregated around the nearest hub airports with a central radiation structure. This gave rise to a rapid increase in the degree of hub nodes, and the entire civil aviation network entered its peak operation period. At noon, routes became denser, and there was a wider node distribution with the highest node degree value compared to other time periods. Although the air transportation network at 18:00 still contained some high-degree nodes, the number of such nodes gradually decreased due to the absence of takeoffs or landings at some small airports, leading to the disconnection of those airports from hub airports. At 24:00, the node distribution of the network was sparse with a small number of travelers, and most departures were from economically developed areas.

The six airports with the highest average node degree value in the air transportation network were Xi’an Xianyang, Beijing Capital, Chengdu Shuangliu, Chongqing Jiangbei, Shanghai Pudong, and Guangzhou Baiyun Airport, with values of 166, 165, 158, 154, 150, and 149, respectively. The high node degree of these airports indicated that they were the most closely connected airports in the air transportation network.

3.2.3. Temporal Property of Average Shortest Path

The average path length of the aviation network can serve as a measure of the convenience of air travel for passengers. From a passenger’s viewpoint, it is often impractical to take two flights within an hour. To evaluate this feature, the authors set the temporal window ω as one year. In the CATN network with a time window of one year, the shortest flight paths are summarized in Table 2. In summary, the average path length in the CATN is 1.97, suggesting that the majority of cities were accessible by changing two or fewer flights. The analysis revealed that 89.75% of city pairs could be reached either through direct flights or with just one flight change.

3.2.4. Temporal Property of Clustering Coefficient

The clustering coefficient is a feature that can be applied to connected graphs. However, when time slicing was applied to the CATN, some graphs in certain time periods became disconnected, which largely consisted of a connected sub-graph and one to three small connected sub-graphs with no more than three airports, which were all branch airports. Hence, the small connected sub-graphs were ignored when calculating the clustering coefficient, and only the maximum connected sub-graph was taken into consideration.

The average clustering coefficient (C) of the network can reflect the overall network characteristics. Figure 7 exhibits that this topological feature demonstrates substantial fluctuations from 6:00 to 9:00 and after 22:00, signifying considerable alterations in the network structure during these periods. The clustering coefficient remained at a high and stable value from 9:00 to 21:00. When combined with the average shortest path, the

CATN demonstrated significant small-world characteristics with high clustering and short distances. The network structure in the early morning consisted of scattered flight routes that did not create a significantly connected sub-graph. As additional airport nodes and flight routes joined the network over time, its structure became increasingly complicated, which resulted in a rapid rise in the clustering coefficient between 5:00 and 7:00, and a subsequent sharp decrease from 7:00 to 9:00. This phenomenon can be attributed to a temporal asymmetry in the rate of growth between routes and airports within the network during distinct time intervals. Specifically, during the period from 5:00 to 7:00, the rate at which routes become part of the network surpasses the rate at which airports are incorporated. In contrast, between 7:00 and 9:00, the rate at which routes integrate into the network lags behind the rate at which airports join.

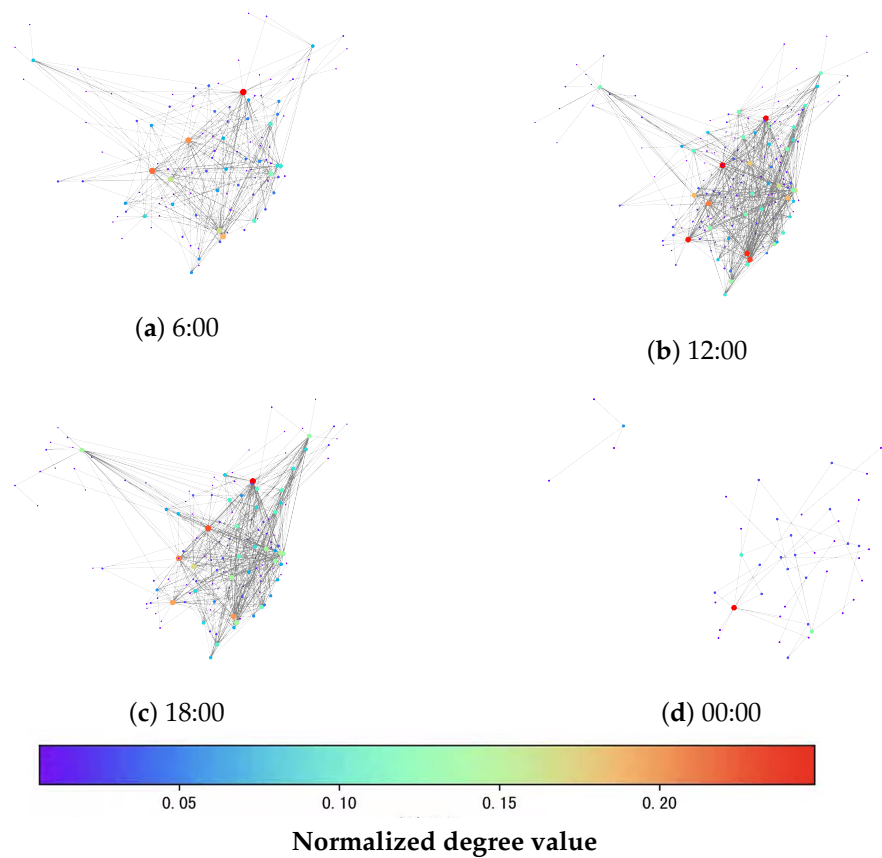


Figure 6. Spatiotemporal features of the aviation network at four specific time intervals. In the provided graph, the size of the nodes corresponds to the degree of those nodes. The color bar in the legend represents different value of normorized degree. Each color corresponds to a specific range of values.

Table 2. Distribution of air routes based on the number of flights.

Shortest Path	Number of Flights Needed to Change	Number of Paths	Percentage of Air Routes
1	0	7156	13.59%
2	1	40,118	76.17%
3	2	5396	10.24%

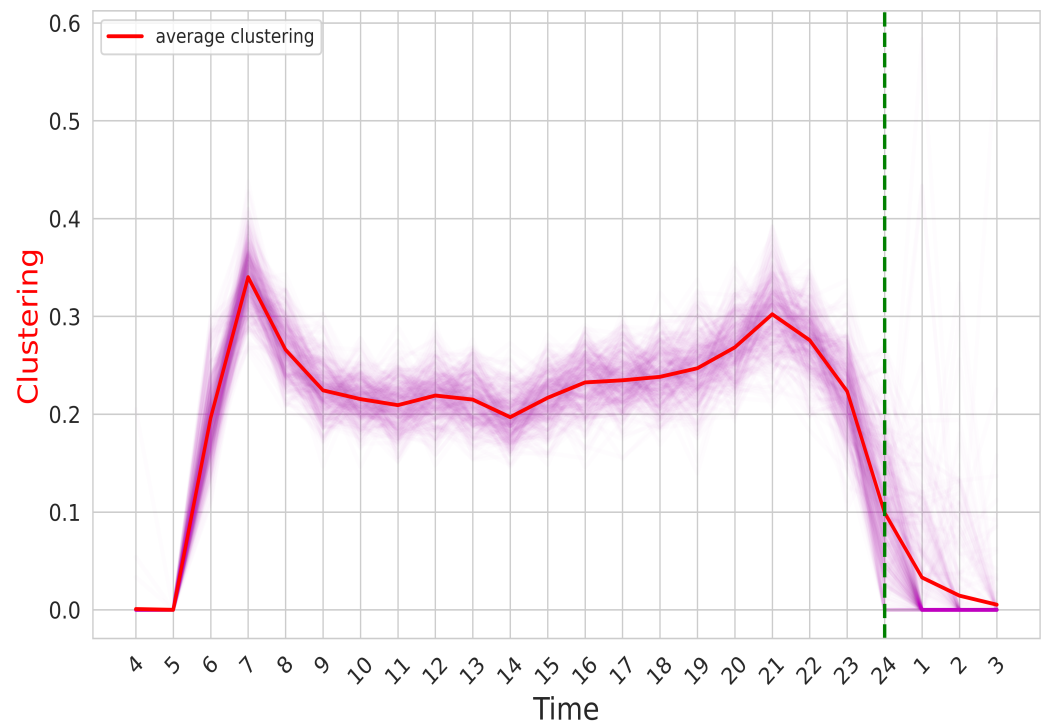


Figure 7. Clustering coefficient in 2018.

The findings of this study revealed the dynamic nature of the network through the examination of the degree and clustering coefficient. The analysis of the temporal and spatial variations in node degree illustrates the dynamic nature of airport operations and the fluctuating distribution of air traffic throughout the day. The fluctuation of the clustering coefficient reflects the changing patterns of connectivity and the growth of the network scale. This provides important data support for airport management and operational optimization, as well as information for the decision-making process of expanding routes and allocating airport resources to ensure effective connectivity and overall transportation performance.

4. Robustness of the CATN

This study investigated four distinct time-stamped versions of the CATN, corresponding to 6:00, 12:00, 18:00, and 24:00. In order to examine the centrality and robustness of the aviation network during these specific time intervals, all flight information from these four time periods in 2018 was combined.

4.1. Estimation of Attack Strategies

Figure 8–11 illustrate the node centrality. The bar chart displays the centrality value of each airport, with the top 15 airports highlighted in blue. Degree centrality distribution was constant over time (Figure 8), which highlighted highly central airports located in hub airports such as Beijing and Shanghai. Airports with a higher nearest neighbor degree centrality are typically regional hub airports, such as provincial capital city airports or economically developed airports. This includes some hub airports with higher degree values, but the nearest neighbor degree of hub airports is generally smaller than that of regional hub airports. Furthermore, the overall nearest neighbor degree exhibits higher values compared to the node degree, implying a dense interconnection among airports and a preference for connecting with hub airports characterized by higher nearest neighbor degrees.

In contrast, the majority of the airports showed low betweenness centrality, with only a few displaying high centrality. These airports likely did not have high degrees, but their

betweenness centrality played a significant role in maintaining network connectivity. Closeness centrality displayed a similar pattern to betweenness centrality, such that the top 15 airports with high betweenness centrality and closeness centrality displayed significant variations over time. In terms of time, the distribution of the CATN appeared to be unbalanced.

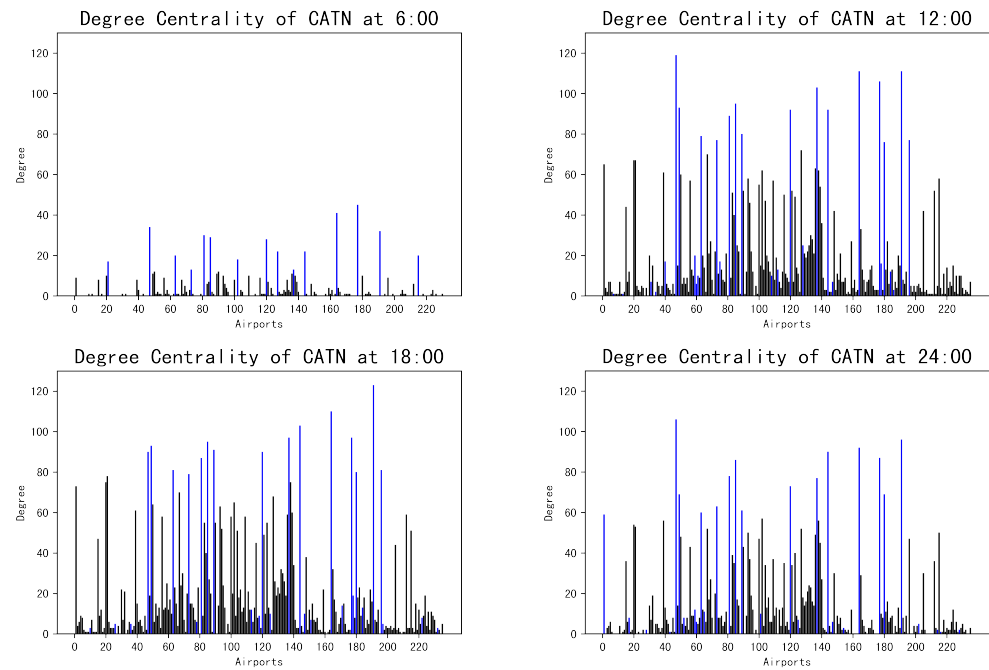


Figure 8. Temporal changes in degree centrality. The blue represent the top 15 airports with high degree centrality. The remaining airports are depicted in black.

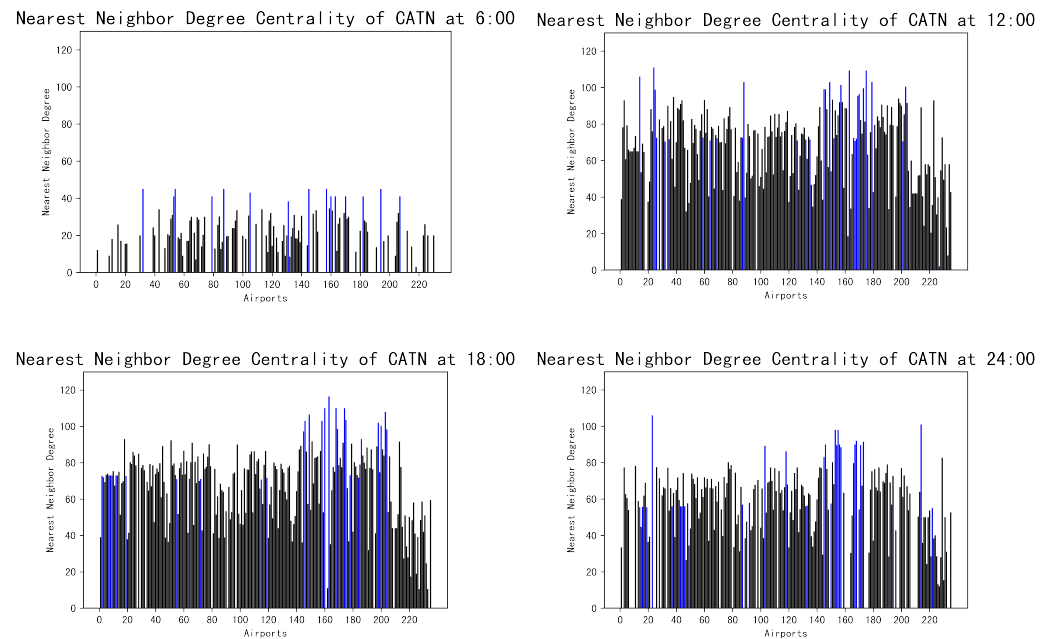


Figure 9. Temporal changes in nearest neighbor degree centrality. The blue represent the top 15 airports with high nearest neighbor degree centrality, while the remaining airports are depicted in black.

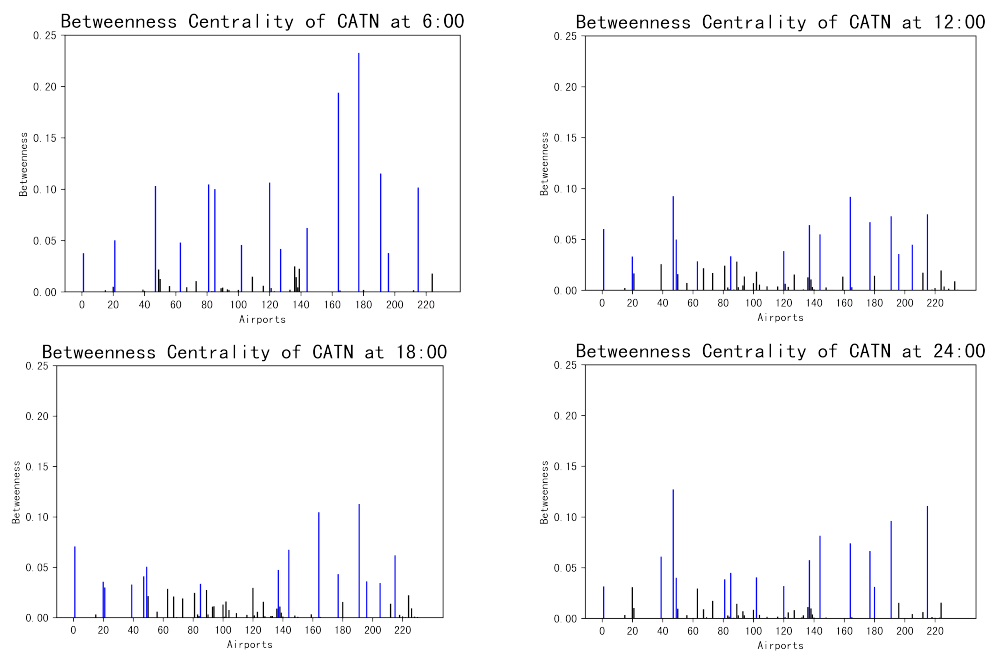


Figure 10. Temporal changes in betweenness centrality. The blue represent the top 15 airports with high nearest neighbor degree centrality, while the remaining airports are depicted in black.

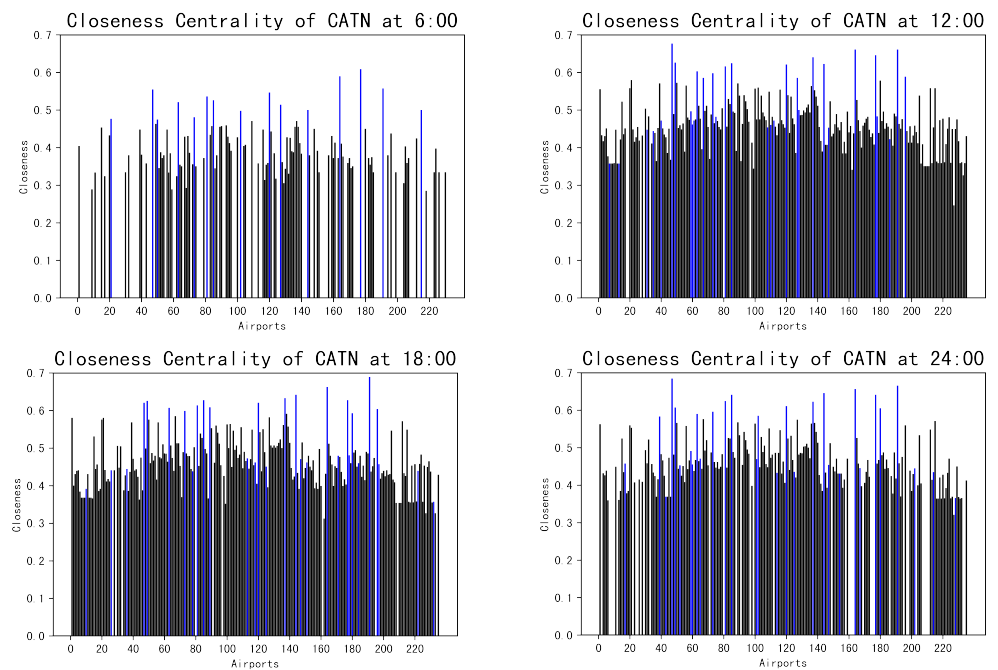


Figure 11. Temporal changes in closeness centrality. The blue represent the top 15 airports with high closeness centrality, while the remaining airports are depicted in black.

4.2. Influence of Structure on CTAN Robustness

This study performed attack experiments on four network snapshots employing centrality metrics as outlined in Section 2. In each experiment, only a single node was targeted, allowing us to investigate the alterations in the maximum connected component when employing both centrality-based and random attack strategies. As the number of deleted nodes increased, the proportion of nodes in the maximum connected component exhibited a significant downward trend (Figure 12). Random attacks were not effective in disrupting the connectivity of the aviation network in all four time intervals. On the

contrary, targeted attacks substantially decreased the connectivity. For instance, when around 10% of the airports were removed, the size of the giant connected component shrunk by 30%, and the network gradually broke down after 20% of the airports were removed.

In comparison to the other four deliberate attack methods, degree-based attacks and nearest neighbor degree attacks had less impact on the robustness of the aviation network. Based on the results of the nearest neighbor degree attacks, an initial sharp decline was observed, indicating the ability of the nearest neighbor degree to rapidly identify crucial nodes in the aviation network, specifically hub airports. However, the subsequent attack effects were not significant and were comparable to random attacks. Referring to the findings in Figure 9, it can be inferred that the nearest neighbor degree attack primarily targets regional hub airports. Although these attacks do not result in a widespread paralysis of the aviation network, the transportation capacity of the network will diminish rapidly. Betweenness and closeness centrality-based attacks were more vulnerable. The uneven temporal distribution of the CATN led to frequent changes in the shortest paths. As both betweenness and closeness centrality indicators were related to the shortest path, safeguarding the hub airports located on the shortest path was necessary to ensure the connectivity of the aviation network.

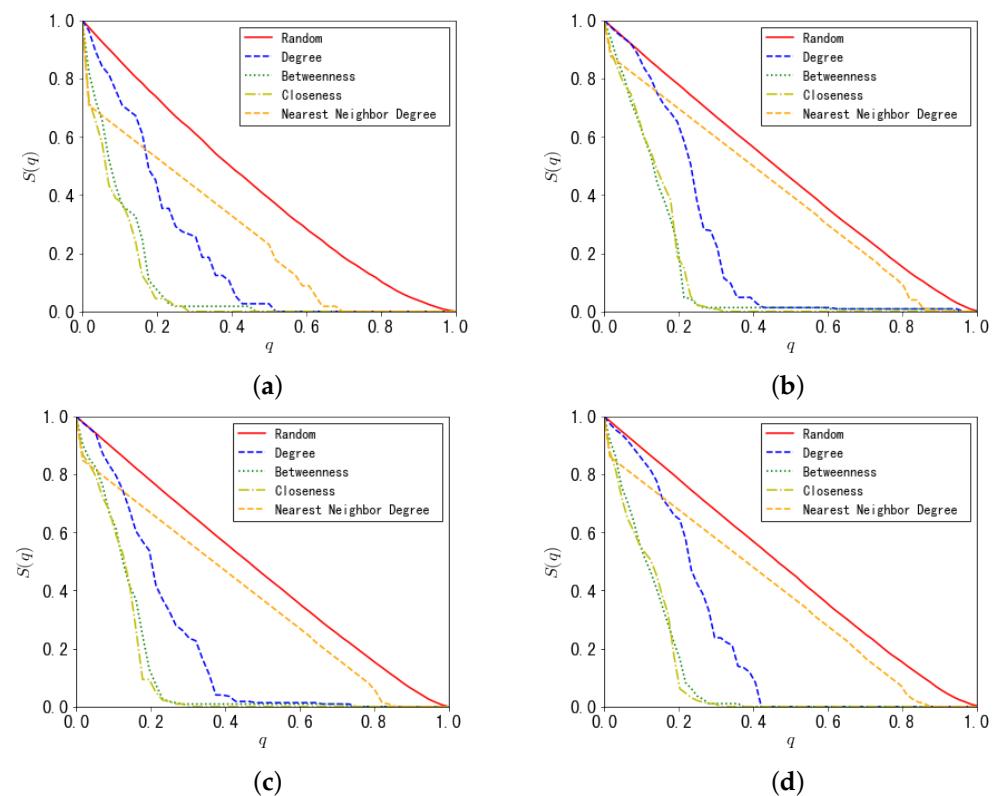


Figure 12. Temporal changes in the size of the maximum connected component in four specific time intervals: (a) the relationship between the relative size of the maximum connected component and the proportion of deleted nodes at 6:00, (b) the relationship between the relative size of the maximum connected component and the proportion of deleted nodes at 12:00, (c) the relationship between the relative size of the maximum connected component and the proportion of deleted nodes at 18:00, and (d) the relationship between the relative size of the maximum connected component and the proportion of deleted nodes at 24:00.

Network efficiency, represented by E , was another indicator for evaluating the robustness of the network under attack. Similar to the analysis conducted on giant components, attacks were carried out by targeting only one node at a time. Specifically, centrality and random attacks were performed on the CATN, and the alterations in CATN efficiency were observed across four time intervals. The attack results are exhibited in Figure 13. Random

attacks were ineffective, so the efficiency did not decrease. Degree-based attacks and nearest neighbor degree attacks produced similar results with the size of the maximum connected component. Betweenness and closeness attacks, however, caused considerable damage to the aviation network. After removing 10% of the airports, the efficiency decreases by nearly 20% of the initial value, and the network gradually collapsed.

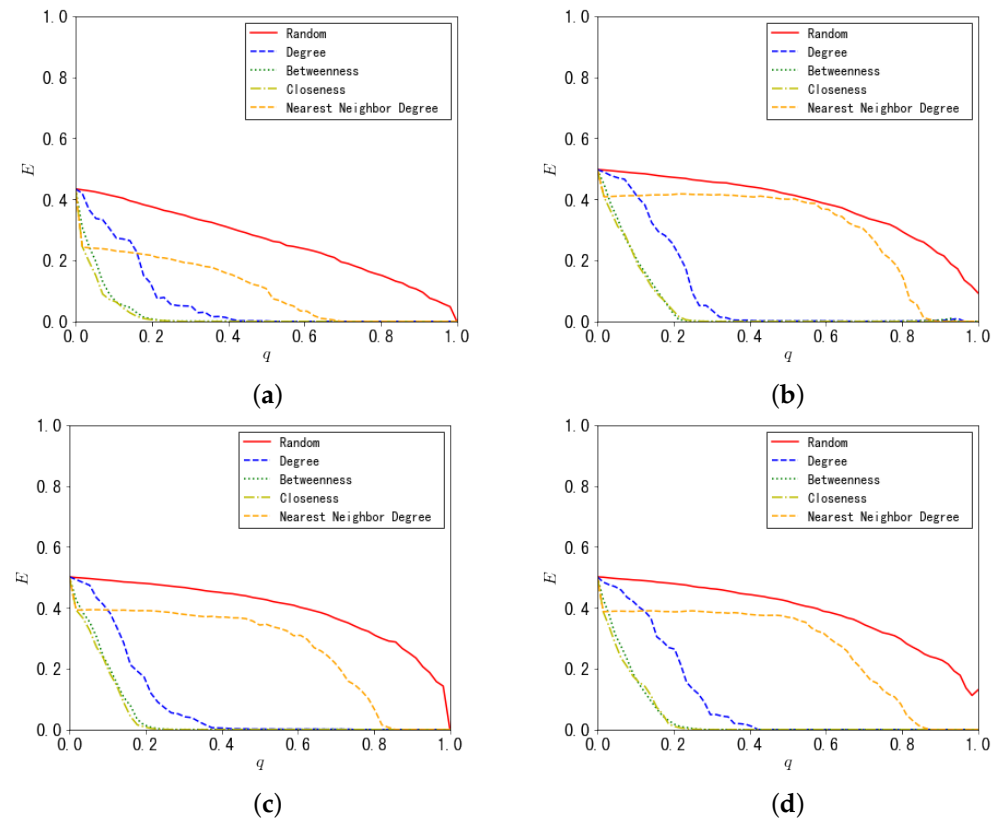


Figure 13. Temporal changes in network efficiency of four specific time intervals: (a) the relationship between weighted network efficiency and the proportion of node removal at 6:00, (b) the relationship between weighted network efficiency and the proportion of node removal at 12:00, (c) the relationship between weighted network efficiency and the proportion of node removal at 18:00, and (d) the relationship between weighted network efficiency and the proportion of node removal at 24:00.

By using the same attack strategy, it was observed that network efficiency was more substantially affected than the maximum connected component. This suggested that, although the aviation network could remain connected with a good network topology after an attack, its efficiency was greatly reduced. As a result, while the aviation network was possibly accessible topologically, it remained disconnected in a temporal sense.

In the aforementioned experiment, the authors employed a single-node attack approach. In order to investigate the network's robustness following attacks on multiple airports, the attack parameters were adjusted to target multiple nodes simultaneously. Specifically, the authors examined the effects of attacking 5 and 10 nodes at once, evaluating their performance based on the proportion of the maximum connected subgraph and network efficiency. The experimental findings, depicted in Figure 14, reveal that, when multiple airports are targeted, the CATN demonstrates substantial resilience against random attacks but exhibits weaker resistance against betweenness and closeness attacks. Consequently, the network's robustness against attack strategies remains comparable to that observed when targeting a single node. Nevertheless, it is notable that both network connectivity and efficiency deteriorate more rapidly.

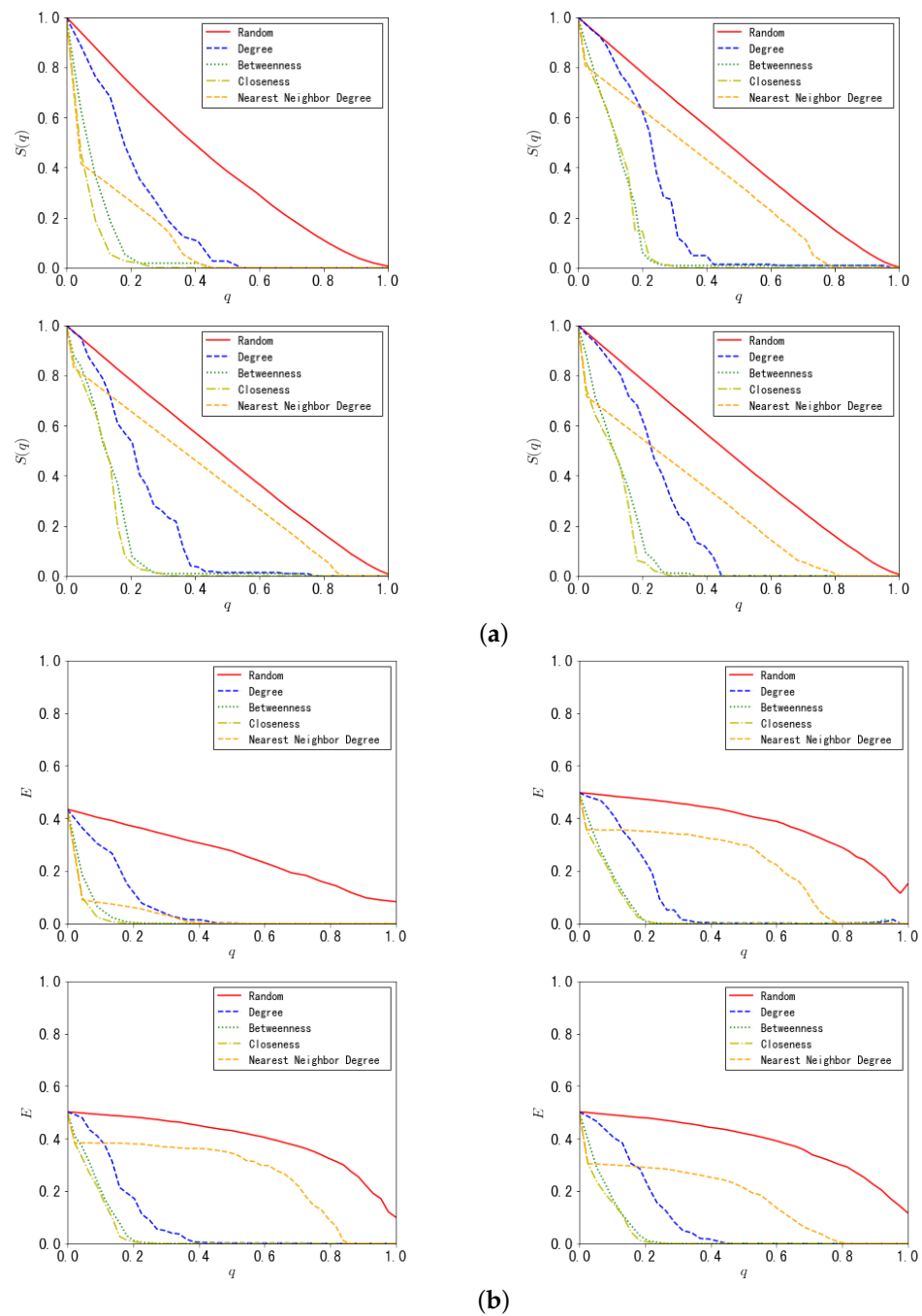


Figure 14. Temporal changes in the size of the maximum connected component and network efficiency of four specific time intervals: (a) attacking 5 nodes at once at 6:00, 12:00, 18:00, and 24:00; (b) attacking 10 nodes at once at 6:00, 12:00, 18:00, and 24:00.

5. Conclusions and Discussion

Complex network and temporal network theories were employed to explore the temporal and topological characteristics of the CATN. The network was defined as a dynamic temporal network and was mapped into a static network using time windows. The results indicated that the aviation network primarily operated from 6:00 to 24:00, with peak hours at 7:00 and 10:00. During these hours, the network exhibited an obvious scale-free characteristic and a small-world phenomenon, with the degree distribution rising rapidly in the initial stages before gradually stabilizing and finally rapidly dropping after the peak hours. Before final stabilization, the distribution of clustering coefficients initially increased and then decreased. The average shortest path showed that 80% of paths passed through

hub airports, with an obvious central radiation structure. Furthermore, the robustness of the CATN at different times against random and deliberate attacks was explored using the proportion of maximum connected sub-graph nodes and network efficiency as robustness measures. The network was weak under deliberate attacks, particularly when using betweenness centrality and closeness centrality strategies. Further, it was observed that the CATN exhibited temporal unevenness in centrality, often leading to changes in the shortest path.

As a preliminary study, the feasibility of temporal network theory in CATN research was verified, and the law of robustness variation in the CATN was discussed. In our future research, an in-depth exploration will be conducted from two perspectives. First, the theory of temporal networks will be employed to investigate the intricate dynamics of networks in the CATN, aiming to provide practical solutions for optimizing flight schedules. This involves addressing cascading failures triggered by nodes or links within the network, as well as the dispersion and propagation of delays. Second, an exploration of more advanced techniques for temporal network modeling will be undertaken, aiming to accurately capture the dynamic structure of the CATN. Event-based temporal networks or dynamic graph neural networks can be utilized for this purpose.

Author Contributions: Conceptualization, R.Y. and W.S.; data curation, W.S.; formal analysis, R.Y.; funding acquisition, H.Z.; methodology, R.Y. and W.S.; resources, R.Y.; supervision, H.Z.; validation, R.Y., M.L. and H.Z.; visualization, W.S.; writing—original draft, R.Y. and W.S.; writing—review & editing, M.L. All authors have read and agreed to the published version of the manuscript.

Funding: This work was supported by the Hainan Provincial Natural Science Foundation of China (grant number 2019RC199) and the National Natural Science Foundation of China (grant number 62167003).

Institutional Review Board Statement: Not applicable.

Informed Consent Statement: Not applicable.

Data Availability Statement: The data and material used in this study were obtained from VariFlight. Due to the commercial nature of the data, access to the data is restricted by the provider. However, we have obtained the necessary permissions and licenses to use the data for our research study.

Acknowledgments: We gratefully acknowledge the financial support provided by the Hainan Provincial Natural Science Foundation of China (grant number 720RC616) and the National Natural Science Foundation of China (grant number 62167003).

Conflicts of Interest: The authors declare no conflict of interest.

Abbreviations

The following abbreviations are used in this manuscript:

CATN	Chinese aviation temporal network
CAN	Chinese temporal network

References

1. Cumelles, J.; Lordan, O.; Sallan, J.M. Cascading failures in airport networks. *J. Air Transp. Manag.* **2021**, *92*, 102026. [[CrossRef](#)]
2. Wang, J.; Bonilla, D.; Banister, D. Air deregulation in China and its impact on airline competition 1994–2012. *J. Transp. Geogr.* **2016**, *50*, 12–23. [[CrossRef](#)]
3. Sallan, J.M.; Lordan, O. *Air Route Networks through Complex Networks Theory*; Elsevier: Exeter Devon, UK, 2019.
4. Mou, J.-H. Analysis of Time Series Network Propagation Dynamics and Its Application in Aviation Networks. Master's Thesis, National University of Defense Technology, Changsha, China, 2017.
5. Chi, L.-P.; Wang, R.; Su, H.; Xu, X.-P.; Zhao, J.-S.; Li, W.; Cai, X. Structural properties of US flight network. *Chin. Phys. Lett.* **2003**, *20*, 1393.
6. Li, W.; Cai, X. Statistical analysis of airport network of China. *Phys. Rev. E* **2004**, *69*, 046106. [[CrossRef](#)]
7. Barrat, A.; Barthélemy, M.; Pastor-Satorras, R.; Vespignani, A. The architecture of complex weighted networks. *Proc. Natl. Acad. Sci. USA* **2004**, *101*, 3747–3752. [[CrossRef](#)]

8. Gautreau, A.; Barrat, A.; Barthélemy, M. Microdynamics in stationary complex networks. *Proc. Natl. Acad. Sci. USA* **2009**, *106*, 8847–8852. [[CrossRef](#)] [[PubMed](#)]
9. Zhang, L.; Du, H.; Zhao, Y.; Maeyer, P.D.; Zhang, X. Drawing topological properties from a multi-layered network: The case of an air transport network in “the belt and road” region. *Habitat Int.* **2019**, *93*, 102044. [[CrossRef](#)]
10. Lordan, O.; Sallan, J.M.; Simo, P.; Gonzalez-Prieto, D. Robustness of the air transport network. *Transp. Res. Part E Logist. Transp. Rev.* **2014**, *68*, 155–163. [[CrossRef](#)]
11. Cong, W.; Hu, M.; Dong, B.; Wang, Y.; Feng, C. Empirical analysis of airport network and critical airports. *Chin. J. Aeronaut.* **2016**, *29*, 512–519. [[CrossRef](#)]
12. Guida, M.; Maria, F. Topology of the Italian airport network: A scale-free small-world network with a fractal structure. *Chaos Solitons Fractals* **2007**, *31*, 527–536. [[CrossRef](#)]
13. Holme, P.; Saramäki, J. *Temporal Network Theory*; Springer: Cham, Switzerland, 2019; Volume 2.
14. Cheng, E.; Grossman, J.W.; Lipman, M.J. Time-stamped graphs and their associated influence digraphs. *Discret. Appl. Math.* **2003**, *128*, 317–335. [[CrossRef](#)]
15. Moody, J. The importance of relationship timing for diffusion. *Soc. Forces* **2002**, *81*, 25–56. [[CrossRef](#)]
16. Bassett, D.S.; Wymbs, N.F.; Porter, M.A.; Mucha, P.J.; Carlson, J.M.; Grafton, S.T. Dynamic reconfiguration of human brain networks during learning. *Proc. Natl. Acad. Sci. USA* **2011**, *108*, 7641–7646. [[CrossRef](#)] [[PubMed](#)]
17. Basu, P.; Bar-Noy, A.; Ramanathan, R.; Johnson, M.P. Modeling and analysis of time-varying graphs. *arXiv* **2010**, arXiv:1012.0260.
18. Isufaj, R.; Koca, T.; Piera, M.A. Spatiotemporal graph indicators for air traffic complexity analysis. *Aerospace* **2021**, *8*, 364. [[CrossRef](#)]
19. Isufaj, R.; Omeri, M.; Piera, M.A.; Valls, J.S.; Gallego, C.E.V. From Single Aircraft to Communities: A Neutral Interpretation of Air Traffic Complexity Dynamics. *Aerospace* **2022**, *9*, 613. [[CrossRef](#)]
20. Kivelä, M.; Cambe, J.; Saramäki, J.; Karsai, M. Mapping temporal-network percolation to weighted, zhestatic event graphs. *Sci. Rep.* **2018**, *8*, 12357 [[CrossRef](#)]
21. Sano, H.H.; Berton, L. A temporal event graph approach and robustness analysis for air transport network. *IEEE Trans. Netw. Sci. Eng.* **2021**, *8*, 3453–3464. [[CrossRef](#)]
22. Holme, P.; Saramäki, J. A map of approaches to temporal networks. In *Temporal Network Theory*; Springer: Cham, Switzerland, 2019; pp. 1–24.
23. George, B.; Shekhar, S. Time-aggregated graphs for modeling spatio-temporal networks. *J. Data Semant.* **2008**, *XI*, 191–212.
24. Ferreira, A. Building a reference combinatorial model for manets. *IEEE Netw.* **2004**, *18*, 24–29. [[CrossRef](#)]
25. Hulovatyy, Y.; Chen, H.; Milenković, T. Exploring the structure and function of temporal networks with dynamic graphlets. *Bioinformatics* **2015**, *31*, 171–180. [[CrossRef](#)]
26. Zhang, J.; Cao, X.-B.; Du, W.-B.; Cai, K.-Q. Evolution of Chinese airport network. *Phys. A Stat. Mech. Appl.* **2010**, *389*, 3922–3931. [[CrossRef](#)] [[PubMed](#)]
27. Liu, H.-K.; Zhang, X.-L.; Zhou, T. Structure and external factors of Chinese city airline network. *Phys. Procedia* **2010**, *3*, 1781–1789. [[CrossRef](#)]
28. Lordan, O.; Sallan, J.M.; Simo, P.; Gonzalez-Prieto, D. Robustness of airline alliance route networks. *Commun. Nonlinear Sci. Numer. Simul.* **2015**, *22*, 587–595. [[CrossRef](#)]
29. Du, W.-B.; Zhou, X.-L.; Lordan, O.; Wang, Z.; Zhao, C.; Zhu, Y.-B. Analysis of the Chinese airline network as multi-layer networks. *Transp. Res. Part E Logist. Transp. Rev.* **2016**, *89*, 108–116. [[CrossRef](#)]
30. Wang, Y.; Zhan, J.; Xu, X.; Li, L.; Chen, P.; Hansen, M. Measuring the resilience of an airport network. *Chin. J. Aeronaut.* **2019**, *32*, 2694–2705. [[CrossRef](#)]
31. Morone, F.; Makse, H.A. Influence maximization in complex networks through optimal percolation. *Nature* **2015**, *524*, 65–68. [[CrossRef](#)]
32. Bai, B. Strategic business management for airport alliance: A complex network approach to simulation robustness analysis. *Phys. A Stat. Mech. Appl.* **2022**, *606*, 126682. [[CrossRef](#)]
33. Latora, V.; Marchiori, M. Efficient behavior of small-world networks. *Phys. Rev. Lett.* **2001**, *87*, 198701. [[CrossRef](#)]
34. Sun, L.; Axhausen, K.W.; Lee, D.H.; Huang, X. Understanding metropolitan patterns of daily encounters. *Proc. Natl. Acad. Sci. USA* **2013**, *110*, 13774–13779. [[CrossRef](#)]

Disclaimer/Publisher’s Note: The statements, opinions and data contained in all publications are solely those of the individual author(s) and contributor(s) and not of MDPI and/or the editor(s). MDPI and/or the editor(s) disclaim responsibility for any injury to people or property resulting from any ideas, methods, instructions or products referred to in the content.